

Article

Test Method for Single Satellite's Inter-Satellite Link Pointing and Tracking via Ground Station

Zhenqiang Hong^{1,2}, Xuxing Huang¹, Lifeng Yang^{1,2}, Zhiqiang Bian^{1,2}, Yong Yang^{1,2} and Shuang Li^{1,*} 

¹ College of Astronautics, Nanjing University of Aeronautics and Astronautics, Nanjing 210016, China; 467998498@qq.com (Z.H.); nuaahxx@nuaa.edu.cn (X.H.); ylfnwpu@126.com (L.Y.); bianzhiqiang2003@163.com (Z.B.); 61803660@qq.com (Y.Y.)

² Shanghai Institute of Satellite Engineering, Shanghai 200240, China

* Correspondence: lishuang@nuaa.edu.cn

Abstract: An inter-satellite link is a key technology that improves control accuracy, transmission efficiency, and autonomous capability of constellations. A satellite's pointing and tracking abilities mainly determine the inter-satellite link's performance, which should be validated through an in-orbit test. However, during the construction of the constellation, the distribution of satellites does not satisfy the constraints of establishing the inter-satellite link. A test method for inter-satellite link pointing and tracking is developed with respect to a single satellite. A practical mission scenario for testing inter-satellite links' performance is constructed. A virtual satellite is introduced as the target satellite to establish an inter-satellite link with the local satellite. The orbit of the virtual target satellite between two ground stations is characterized based on the Newton–Raphson method. By comparing the predicted and actual time differences between two ground stations receiving the signals from the local satellite, the inter-satellite link pointing and tracking abilities are evaluated independently. Numerical simulations verify the design of the virtual satellite. The single satellite test method for inter-satellite link pointing and tracking abilities is available.

Keywords: virtual satellite; inter-satellite link; pointing and tracking; in-orbit test; ground station



Citation: Hong, Z.; Huang, X.; Yang, L.; Bian, Z.; Yang, Y.; Li, S. Test Method for Single Satellite's Inter-Satellite Link Pointing and Tracking via Ground Station. *Aerospace* **2024**, *11*, 713. <https://doi.org/10.3390/aerospace11090713>

Academic Editor: Fanghua Jiang

Received: 18 June 2024

Revised: 23 August 2024

Accepted: 28 August 2024

Published: 31 August 2024



Copyright: © 2024 by the authors. Licensee MDPI, Basel, Switzerland. This article is an open access article distributed under the terms and conditions of the Creative Commons Attribution (CC BY) license (<https://creativecommons.org/licenses/by/4.0/>).

1. Introduction

In recent years, heterogeneous constellations [1], including SpaceX's Starlink, have developed rapidly. The heterogeneous constellations are composed of several sub-constellations at different orbital altitudes. The heterogeneous constellations provide network services to the whole world. Also, they can be used as measurement and control terminals to effectively alleviate shortages of ground-based measuring and control resources [2]. As a transmission bridge between satellites in the constellations, an inter-satellite link is one of the key technologies in space-based information networks [3].

Inter-satellite link technology is essential for improving the accuracy, efficiency, and autonomous capability of a multi-satellite system, such as a global navigation system. After the construction of inter-satellite links throughout the entire constellation, high-accuracy orbital parameters can be autonomously broadcast in the system. Chen et al. [4] and Li et al. [5] proposed efficient measuring methods for multi-layer constellations using an inter-satellite link. Lin et al. improved the navigation accuracy by updating the ephemeris frequently [6]. The ephemeris can be injected using the inter-satellite link of the constellation. Meanwhile, inter-satellite link technology can improve autonomous navigation performance with respect to user terminals in complex environments. Lin et al. [7], Fernandez [8], and Zhang et al. [9] studied completely autonomous navigation technologies. Traditional ground infrastructures can be replaced by inter-satellite links, which further reduce the operation cost. Moreover, the inter-satellite link can be employed in other applications. Xie et al. estimated the yaw angle of a satellite using an inter-satellite link [10]. Without introducing new parameters, the estimation accuracy can be improved by adding

redundant observations. Zhang et al. eliminated the effect of empirical weight on the fusion data processing, thereby increasing the orbit determination accuracy [11]. Kur et al. [12] and Michalak et al. [13] studied high-precision clock synchronous correction methods. According to previous studies, a precondition for employing an inter-satellite link is that the link equipment of the constellations is in a consistent state, which guarantees continuity and reliability. Therefore, high-confidence verifications of the performance of an inter-satellite link should be conducted. However, current studies do not involve an efficient in-orbit test method for the performance of a constellation's inter-satellite link, especially when the constellation is still under construction. This restricts the rapid iteration and further development of the inter-satellite link technology for mega-constellations.

In practical missions, the in-orbit test of an inter-satellite link's performance concentrates on the pointing and tracking abilities of a satellite in an operation state. Typical inter-satellite link transmission mainly involves microwave and laser equipment, which are widely used for data projection and relay [14,15]. The microwave beam is wide, but the transmission rate is low [16–18]. Laser beams show high-speed and strong anti-interference ability, enabling efficient and accurate transmissions between satellites. The test methods for this equipment have been studied. Schlicht et al. completed the test of orbit determination for the Galileo spacecraft based on two-way laser inter-satellite links [19,20]. The results show that the orbit determination efficiency via an inter-satellite link is related to the visibility of the other satellites in the constellation. Scheinfeild et al. analyzed multiple search methods, such as scan/gaze and scan/scan [21]. The influences of a satellite's structural vibration on the inter-satellite links were studied. A compensatory method was then developed to eliminate deviations between the pointing vectors of the transmitter and the receiver telescope. To achieve high-accuracy signal capture and tracking, both the microwave and laser in the above research required the altitude of the satellite to calculate the inter-satellite link pointing angle [21,22]. In-orbit tests are carried out accordingly [23]. Teng et al. studied the method of calculating the pointing angles of transmission devices based on the topology architecture and routing of the constellation and the ephemeris of the satellite. The solutions for the pointing angles are uploaded to the spaceborne computer and executed. By comparing the in-orbit results and the calculation results, the performance of the pointing and tracking are validated. The review by Lin et al. carried out recapture studies on inter-satellite laser links, considering a pointing error model of multipoint link terminals [24]. The results showed that subsequent research on inter-satellite links should optimize the scanning capture parameters of inter-satellite laser links.

Current studies on the in-orbit test methods for inter-satellite links' performance highlight constellations that have been constructed. However, the construction of mega-constellations always takes several years [25,26]. During the construction of the constellation, due to the loose distribution of the satellites, the distance and visibility between satellites might not satisfy the constraints for establishing an inter-satellite link [27]. Meanwhile, an inter-satellite link's performance should be tested in advance so that the construction of the constellation can be more flexible and confident. Therefore, the test method for a single satellite's pointing and tracking abilities has potential in practical missions.

In this paper, a ground-station-based high-confidence test method for inter-satellite link pointing and tracking performances with respect to a single satellite is developed. During the construction of the constellation, due to the insufficiency of inter-satellite linking resources, the pointing and tracking abilities of the in-orbit satellite cannot be tested immediately. The ground station has the ability to construct a link with the in-orbit satellite, which can be employed to simulate the inter-satellite transmission. The test for a single satellite's pointing and tracking abilities involves using multiple ground stations. The contributions of this paper are summarized as follows: (1) A practical mission scenario for testing an inter-satellite link's performance is established. A local satellite and a target satellite are introduced as a signal projector and receiver, respectively. The motion of the beam of the local satellite during the tracking is described by the rotation angle and the off-axis angle. (2) A virtual target satellite for testing an inter-satellite link is proposed.

The signal-receiving process of the virtual satellite is simulated by two ground stations. The orbit of the virtual satellite is analytically derived. The time difference between two transmissions with different ground stations is solved based on a Newton–Raphson method. (3) A test method for inter-satellite link pointing and tracking is proposed. Based on the virtual target satellite, the corresponding rotation angles, and off-axis angles with respect to the ground stations are obtained. During the inter-satellite link test, considering the time difference between ground stations receiving the signals from the local satellite, the inter-satellite link pointing and tracking abilities are evaluated.

The rest of this paper is organized as follows: Section 2 presents the models of pointing vectors and pointing angles for establishing an inter-satellite link. In Section 3, the design method for a virtual target satellite via two ground stations is developed. The test method for inter-satellite link pointing and tracking is provided. The design of the virtual satellite and the test method for its pointing and tracking abilities are validated through numerical simulations in Section 4. Finally, Section 5 draws a conclusion of this paper.

2. Models of Inter-Satellite Link Pointing and Tracking

2.1. Pointing Vector Calculation

The inter-satellite link transmits data between satellites, which can be simplified as multiple pointing vectors from point to point in the constellation. These pointing vectors are the relative position vectors from a local satellite with a projector to another target satellite with a receiver. By propagating the orbits of both satellites, the pointing needed to maintain the transmissions of the inter-satellite link can be calculated.

In the present study, the inter-satellite link vector pointing from the local satellite to the target satellite in the J2000 geocentric inertial frame of reference is r_{link}^i , in the orbital frame is r_{link}^o , in the satellite body frame is r_{link}^b , and in the antenna frame is r_{link}^a . The transforms between coordinate frames are shown as follows:

$$r_{link}^a = A_{ab}r_{link}^b = A_{ab}A_{bo}r_{link}^o = A_{ab}A_{bo}A_{oi}r_{link}^i \tag{1}$$

where A_{ab} is the transformation matrix from the satellite body frame to the antenna frame; A_{bo} is the transformation matrix from the satellite orbital frame to the satellite body frame; and A_{oi} is the transformation matrix from the J2000 inertial frame to the satellite orbital frame.

Then, the position vector in the J2000 inertial frame of reference from the Earth’s center to the local satellite is r_{local}^i , and the velocity vector of the local satellite is v_{local}^i . The vectors of the local satellite orbital frame reference are

$$\begin{cases} Z_o = -\frac{r_{local}^i}{|r_{local}^i|} \\ Y_o = -\frac{r_{local}^i \times v_{local}^i}{|r_{local}^i \times v_{local}^i|} \\ X_o = Y_o \times Z_o \end{cases} \tag{2}$$

Following these vectors, the transformation matrix from the inertial frame to the orbital frame A_{oi} is given as

$$A_{oi} = [X_o^T \ Y_o^T \ Z_o^T]^T \tag{3}$$

The transformation matrix from the satellite orbital frame to the satellite body frame is A_{bo} given as in Equations (4) and (5), where φ , θ , and ψ are the roll, pitch, and yaw angles of the satellite body frame relative to the satellite orbital frame, respectively.

$$A_{bo} = A_y(\theta)A_x(\varphi)A_z(\psi) \tag{4}$$

$$A_y(\theta) = \begin{bmatrix} \cos \theta & 0 & -\sin \theta \\ 0 & 1 & 0 \\ \sin \theta & 0 & \cos \theta \end{bmatrix}, A_x(\varphi) = \begin{bmatrix} 1 & 0 & 0 \\ 0 & \cos \varphi & \sin \varphi \\ 0 & -\sin \varphi & \cos \varphi \end{bmatrix}, A_z(\psi) = \begin{bmatrix} \cos \psi & \sin \psi & 0 \\ -\sin \psi & \cos \psi & 0 \\ 0 & 0 & 1 \end{bmatrix} \tag{5}$$

The position vector of the target satellite in the J2000 inertial frame r_{tag}^i and r_{link}^i can be expressed as follows:

$$r_{link}^i = \frac{r_{tag}^i - r_{local}^i}{|r_{tag}^i - r_{local}^i|} \tag{6}$$

2.2. Beam Pointing Angle

Beam pointing is the instantaneous vector of a microwave antenna or a laser link. As the relative position of the constellation evolves, the pointing is time-varying. In this situation, in order to maintain the inter-satellite link, the line of sight (LOS) of the beam point should track the target satellite. The beam-pointing vector in the antenna coordinate frame $[X_a, Y_a, Z_a]$ is converted by two beam-pointing angles, the rotation angle and the off-axis angle in Figure 1 and Equations (7) and (8). The corresponding range of the off-axis angle is $[0, \pi/2]$, and the range of the rotation angle is $[0, 2\pi]$.

$$\gamma_{oa} = \arccos\left(\frac{z_a}{\|r_{link}^a\|}\right), r_{link}^a = [x_a \ y_a \ z_a]^T, \gamma_{oa} \in [0, \pi/2] \tag{7}$$

$$\gamma_{ra} = \begin{cases} \arctan2(y_a, x_a), & y_a \geq 0 \\ \arctan2(y_a, x_a) + 2\pi, & y_a < 0 \end{cases}, \gamma_{ra} \in [0, 2\pi] \tag{8}$$

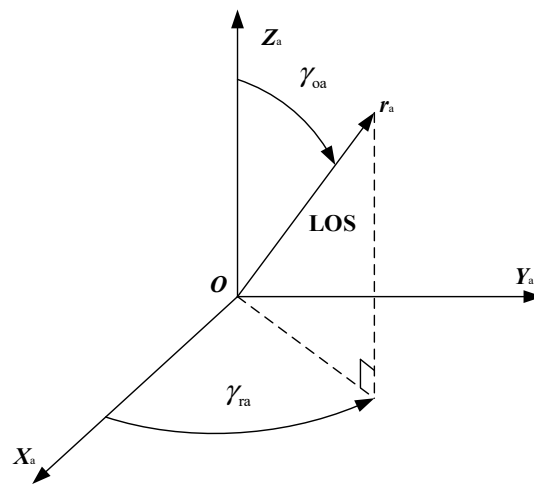


Figure 1. Definition of the link beam pointing angle. γ_{oa} denotes the off-axis angle; γ_{ra} denotes the rotation angle.

3. Inter-Satellite Links Pointing and Tracking in-Orbit Test Method

3.1. Test Method for Single Satellite’s Inter-Satellite Link Pointing and Tracking

In order to validate the performance of the inter-satellite link in the current test method, the local satellite points and tracks an in-orbit target satellite. However, during the construction of the constellation, the distribution of the satellites might not satisfy the constraints for testing the inter-satellite link. In the present paper, an indirect test method for inter-satellite link pointing and tracking based on ground stations and a virtual satellite is developed. This indirect test process is shown in Figure 2.

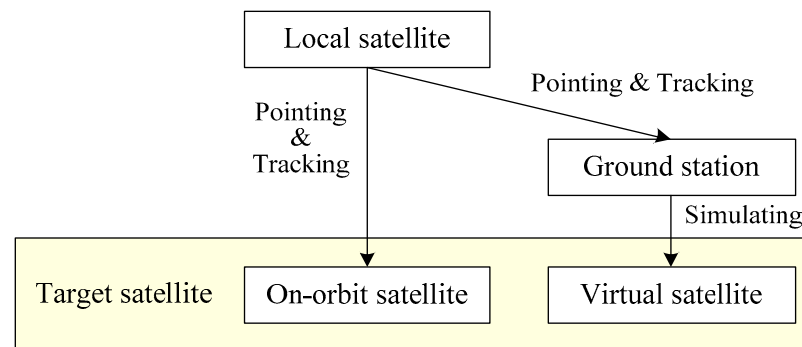


Figure 2. Indirect test process for single satellite's inter-satellite links pointing and tracking.

Due to the lack of an in-orbit target satellite, the ground stations are introduced to simulate the positions of the virtual target satellite. The ground stations have capacities for receiving signals from the local satellite and calculating the time difference in signal reception between the two ground stations. Therefore, by pointing and tracking two ground stations, the local satellite indirectly validates the process of tracking the target satellite. In this situation, the corresponding orbit of the virtual target satellite is generated according to the visibilities between the local satellite and the ground stations. A detailed design method for the virtual satellite is provided in Section 3.2.

Based on the ground station and the virtual satellite, the basic flow of the indirect test method is shown in Figure 3. The test method for inter-satellite link pointing and tracking is divided into the following steps:

- (1) Choose two ground stations: A and B. Set time t_1 when the local satellite points to ground station A, according to practical requirements. Then, propagate the positions of the ground stations r_d at time t_1 ;
- (2) Calculate the position of the local satellite r_s and the relative positions between the local satellite and the ground stations r_{dAs} , r_{dBs} . The positions $r_A(t_1)$ and $r_B(t_1)$ of the virtual target satellites with respect to ground stations A and B, respectively, are obtained at time t_1 ;
- (3) Calculate the time t_2 when the local satellite points to ground station B and the corresponding position $r_B(t_2)$ of the virtual target satellite, based on a Newton iteration method. The time difference between pointing to ground stations A and B is obtained. A detailed method is provided in Section 3.3;
- (4) Calculate the velocity of the virtual target satellite v_A . The orbit of the virtual target satellite is obtained. A detailed calculation method is provided in Section 3.4;
- (5) Predict the time difference between two ground stations receiving the signals from the local satellite. Then, the pointing and tracking of the local satellite with respect to the ground stations is executed in-orbit. The actual time difference is also obtained. By comparing the actual time difference and predicted time difference, the inter-satellite link pointing and tracking abilities of the local satellite are verified.

Moreover, in order to test the inter-satellite link pointing and tracking performance, the virtual satellite should be similar to a practical satellite. Therefore, taking a practical constellation as a reference, the orbital altitude h_0 of the virtual target satellite is set the same as the practical satellite to establish the inter-satellite link. The eccentricity is set as 0. Other orbital elements, including the right ascension of the ascending node, the argument of perigee, and the true anomaly, are solved by iterating steps (3)–(4). The orbital period of the virtual target satellite is denoted as T_0 . The angular velocity can be obtained as $2\pi/T_0$.

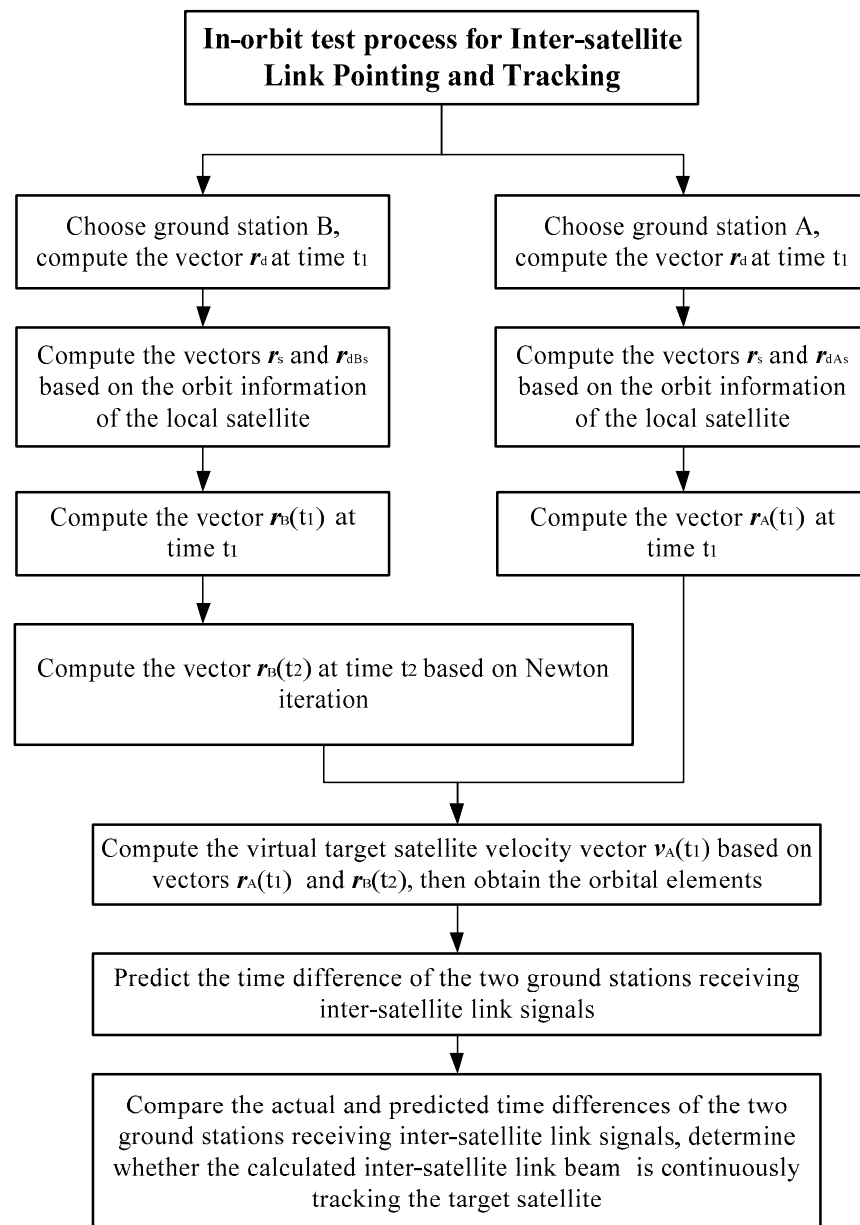


Figure 3. Test method for inter-satellite link pointing and tracking.

While tracking the virtual target satellite, when the beam points to the virtual target satellite and ground station simultaneously, the single local satellite transmits signals to ground stations A and B. In this situation, a high-confidence test for a single satellite's inter-satellite link pointing and tracking can be executed. Note that in practical missions, for inter-satellite links with larger beam angles, the time needed for constructing a link to the ground station is longer; for laser inter-satellite links, the link-construction time is shorter. The proposed method can test both kinds of link pointing.

3.2. Virtual Target Satellite Based on Ground Stations

In the present paper, the inter-satellite link pointing and tracking performance is tested using a virtual target satellite. A practical way to generate a virtual target satellite is by simulating the signal-receiving process and forming a virtual orbit around two ground stations. The geometry of the inter-satellite link via the virtual satellite is shown in Figure 4.

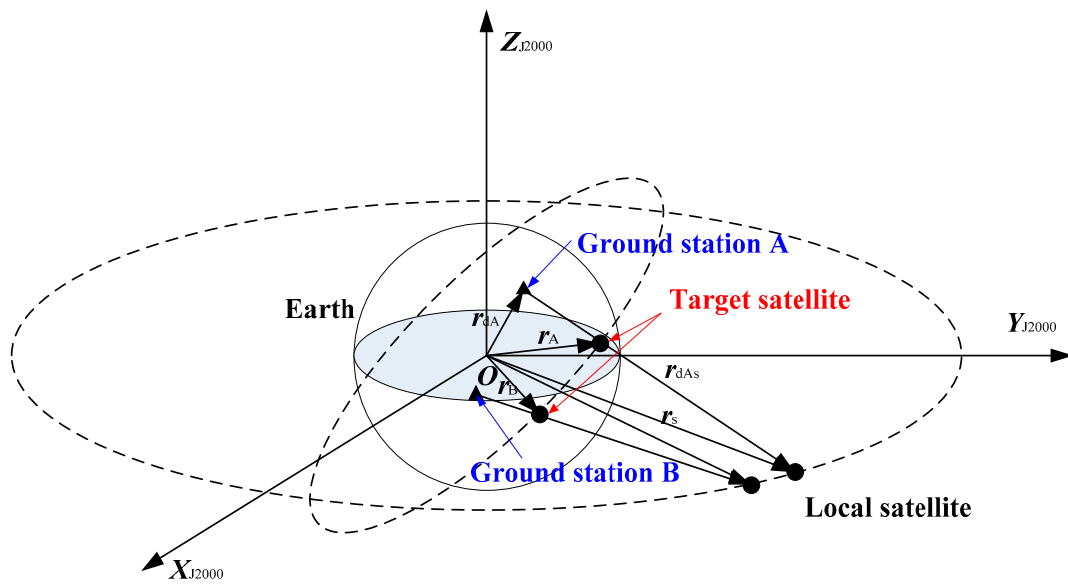


Figure 4. Schematic diagram of the inter-satellite link between the two satellites in-orbit.

In Figure 4, the ground stations are defined as A and B to simulate the virtual target satellite orbit. Taking ground station A as an example, the position vector of ground station A r_{dA} in the Earth-fixed coordinate system is given as follows:

$$r_{dA} = \begin{bmatrix} (H + h) \cos \varepsilon \cos \lambda \\ (H + h) \cos \varepsilon \sin \lambda \\ [(1 - e_E^2)H + h] \sin \varepsilon \end{bmatrix} \quad (9)$$

where λ , ε , and h denote the longitude, latitude, and altitude of the ground station, respectively, and $e_E = 0.08182$ is the oblateness of the Earth. H is denoted as follows:

$$H = \frac{R_e}{\sqrt{1 - e_E^2 \sin^2 \varepsilon}} \quad (10)$$

where R_e is the radius of the Earth, and $R_e = 6378.145$ km.

Then, the position vector of the ground station $r_d(t_1)$ in the J2000 geocentric inertial frame at time t_1 is obtained as follows:

$$r_d(t_1) = A_{ie}(t_1) r_{dAs} \quad (11)$$

where $A_{ie}(t_1)$ defines the transformation from the Earth-fixed coordinate frame to the J2000 geocentric frame.

Meanwhile, the position vector of the local satellite in the J2000 geocentric frame at time t_1 is shown as follows:

$$r_s(t_1) = \begin{bmatrix} r(\cos u \cos \Omega - \sin u \cos i \sin \Omega) \\ r(\cos u \sin \Omega + \sin u \cos i \cos \Omega) \\ r \sin u \sin i \end{bmatrix} \quad (12)$$

where a , e , i , Ω , ω , and f represent the semi-major axis, eccentricity, inclination, right ascension of ascending node, argument of perigee, and true anomaly of the local satellite, respectively; u represents the argument of latitude, $u = \omega + f$; and r represents the geocentric distance of the local satellite, $r = \frac{p}{1 + e \cos f}$, $p = a(1 - e^2)$.

The relative position r_{dAs} from the ground station A to the local satellite in the J2000 geocentric frame at time t_1 can be calculated as follows:

$$r_{dAs}(t_1) = r_s(t_1) - r_{dA}(t_1) \quad (13)$$

Then, as shown in Figure 4, in order to simulate the position of the virtual target satellite using a ground station, the local satellite should be simultaneously linked to the ground station and the virtual satellite. In this situation, the local satellite, the virtual target satellite, and the ground station should be triple-collinear as follows:

$$k^2 \cdot r_{dAs}^2(t_1) + r_{dA}^2(t_1) + 2k \cdot r_{dAs}(t_1)r_{dA}(t_1) = r_A^2(t_1) \quad (14)$$

where h_o denotes the orbital altitude of the virtual target satellite; $r_A(t_1)$ denotes the position vector of the virtual satellite in the J2000 geocentric frame at time t_1 ; and $k > 0$.

In addition, it should be emphasized that in practical missions, the beam of the local satellite's antenna is a cone with a small angle. In this situation, the ground station can still receive the signal from the local satellite for an extended period.

To solve Equation (14), the parameters are defined as follows:

$$\begin{cases} a_1 = r_{dAs}^2(t_1) \\ a_2 = 2k \cdot r_{dAs}(t_1)r_{dA}(t_1) \\ a_3 = r_{dA}^2(t_1) - r_A^2(t_1) \end{cases} \quad (15)$$

The solution of Equation (14) can be derived as:

$$k = \frac{-a_2 + \sqrt{a_2^2 - 4a_1a_3}}{2a_1} \quad (16)$$

According to the geometry, the space vector pointing from the geocentric to the virtual target satellite at time t_1 in the J2000 coordinate system is obtained as follows:

$$r_A(t_1) = r_{dA}(t_1) + k \cdot r_{dAs}(t_1) \quad (17)$$

For the ground station B, the same algorithm is used:

$$r_B(t_1) = r_{dB}(t_1) + k \cdot r_{dBs}(t_1) \quad (18)$$

where $r_{dB}(t_1)$ represents the position vector of station B in the J2000 geocentric frame at time t_1 ; and $r_{dBs}(t_1)$ represents the relative position vector from the ground station B to the local satellite.

3.3. Time Difference in Tracking Based on Newton–Raphson Method

According to the test process for a single satellite's inter-satellite link pointing and tracking, the local satellite first points to ground station A at time t_1 and then points to ground station B at time t_2 . Since the maneuvers of the antenna and the altitude of the satellite are not instantaneous, the time difference Δt between the local satellite points to ground station A and to ground station B should be considered, $\Delta t = t_2 - t_1$. The Newton–Raphson method is employed to calculate the time when the local satellite points to the ground station B t_2 and the time difference Δt . Then, the position vector of the virtual target satellite $r_B(t_2)$ at time t_2 is propagated.

The Newton–Raphson method is a typical root-finding algorithm that solves the next value using current values. The main steps of the Newton–Raphson method are as follows:

- (1) Determine the iteration variable;
- (2) Establish an iterative relationship by recursion or by working backward;
- (3) Set a fixed number of loops to end the iterative process to achieve control of the iterative process.

Based on the Newton–Raphson method, an iterative method to solve the position vector $\mathbf{r}_B(t_2)$ of the virtual satellite at time t_2 and the time difference $\Delta t = t_2 - t_1$ is developed. The initial time of t_2 is set as the time t_1 . In this situation, the position of the virtual target satellite is obtained as $\mathbf{r}_B(t_1)$. The time difference Δt of the virtual target satellite from $\mathbf{r}_A(t_1)$ to $\mathbf{r}_B(t_1)$ can be calculated as follows:

$$\Delta t = \arccos\left(\frac{\mathbf{r}_A(t_1) \cdot \mathbf{r}_B(t_1)}{|\mathbf{r}_A(t_1)| \cdot |\mathbf{r}_B(t_1)|}\right) \cdot \frac{T_o}{2\pi} \quad (19)$$

Subsequently, a new position $\mathbf{r}_B'(t_1 + \Delta t)$ is obtained using the time difference Δt . Based on the Newton–Raphson method, the position of the virtual satellite is iteratively updated from $\mathbf{r}_B(t_1)$ to $\mathbf{r}_B(t_2)$ until the time difference Δt converges at a fixed value. Meanwhile, considering both the computation efficiency and position accuracy, a fixed number of loops is set as five. After five iterations, the convergence error of time t_2 is about 10^{-5} – 10^{-7} s (based on the altitudes of local and target satellites), which is observable in practical missions.

3.4. Characterization of Virtual Target Satellite Orbit Based on Double Vectors

In order to solve the orbital parameters of the virtual target satellite, a characterization method is provided using the position and velocity at a particular moment.

For circular orbits, based on the orbital altitude and angular velocity, the norm of flight velocity of the virtual target satellite is given as follows:

$$|v_A(t_1)| = \frac{2\pi}{T_o}(R_e + h_o) \quad (20)$$

The direction of the velocity vector $\mathbf{v}_A(t_1)$ of the virtual target satellite at time t_1 in the J2000 is obtained using the cross product of position vectors $\mathbf{r}_A(t_1)$ and $\mathbf{r}_B(t_1)$. The angular momentum vector \mathbf{r}_n is denoted as:

$$\mathbf{r}_n = \frac{\mathbf{r}_A(t_1) \times \mathbf{r}_B(t_2)}{|\mathbf{r}_A(t_1) \times \mathbf{r}_B(t_2)|} \quad (21)$$

According to triangulation theory, the position vectors of the ground stations $\mathbf{r}_A(t)$ and $\mathbf{r}_B(t)$ should be non-collinear. The velocity vector of the virtual target satellite at time t_1 is obtained as

$$\mathbf{v}_A(t_1) = \frac{\mathbf{r}_n \times \mathbf{r}_A(t_1)}{|\mathbf{r}_n \times \mathbf{r}_A(t_1)|} \cdot \frac{2\pi}{T_o}(R_e + h_o) \quad (22)$$

Using the satellite position vector and the velocity vector at the time t_1 , the orbital parameters of the virtual target satellite orbits can be obtained.

4. Numerical Simulation

4.1. Validation of Virtual Satellite with Respect to the Ground Stations

In this section, the proposed ground station-based test method for inter-satellite link pointing and tracking is validated and evaluated.

The behavior of the virtual satellite with respect to the ground stations is first validated. A single satellite test scenario for inter-satellite link pointing and tracking is established. The longitudes, latitudes, and altitudes of the ground stations are listed in Table 1. The mission epoch is set as 5:00 a.m. (UTC) on 1 September 2023. The local satellite is located in a geostationary orbit with a longitude of 100° E. The orbital altitude of the virtual target satellite is set as 600 km. The pointing vectors and time difference are calculated accordingly.

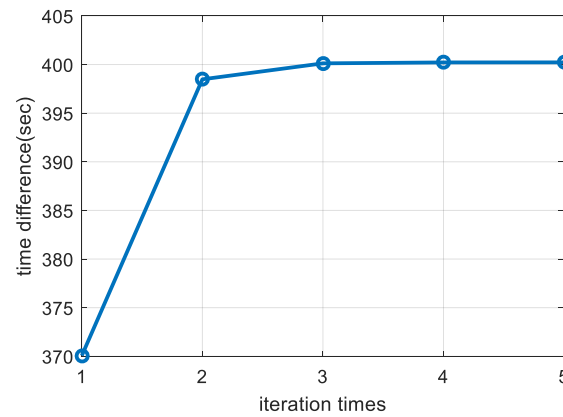
Table 1. Locations of the two ground stations.

Geographic Information	Ground Station A	Ground Station B
latitude	35° N	30° N
longitude	90° E	120° E
altitude	150 m	0 m

Following the simulation conditions and the Newton–Raphson method, the orbital parameters of the virtual satellite are obtained as follows:

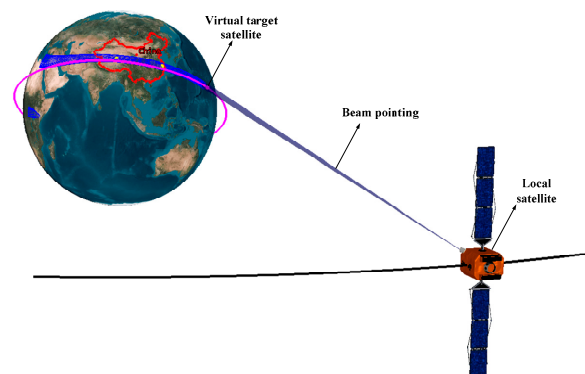
$$a = 6978 \text{ km}, e = 0, i = 30.9103^\circ, \Omega = 50.6987^\circ, \omega = 79.2623^\circ, f = 15.4974^\circ \quad (23)$$

The iterative convergence curve is shown in Figure 5. The time difference Δt converges to 400.1 s after five iterations. The final error of the time difference is 5 ms. The results demonstrate that the proposed method can simulate the position of the virtual satellite using two ground stations.

**Figure 5.** Newton–Raphson method convergence curve of the time difference in the target satellite passing above ground stations A and B.

4.2. Validation of Inter-Satellite Links Pointing and Tracking

Based on the virtual target satellite in Section 3.2, the test method for inter-satellite link pointing and tracking is validated. The half angle of the beam is set as 0.3° . The ground stations receive the inter-satellite link signals from the local satellite. The orbit of the local satellite and the ground projection of the beam pointing are shown in Figures 6 and 7, respectively. The time durations of the inter-satellite links pointing to the ground stations are shown in Figure 8 and Table 2.

**Figure 6.** Inter-satellite link pointing in the 3D scene.

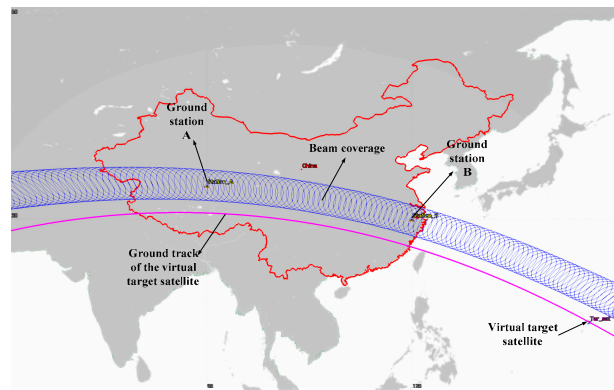


Figure 7. Ground projection of inter-satellite link of the local satellite.

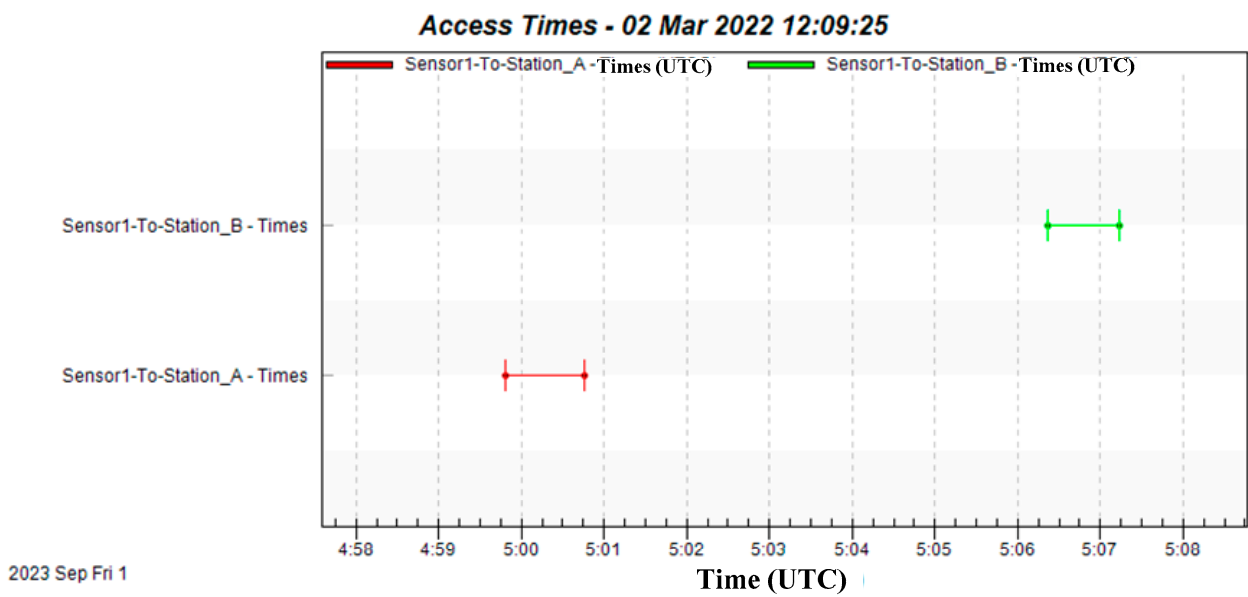


Figure 8. Signal reception time of ground stations during tracking of inter-satellite links.

Table 2. The time duration of the inter-satellite links pointing to different ground stations during tracking.

Ground	Starting Time	Ending Time	Duration
A	1 September 2023-04:59:48.674	1 September 2023-05:00:45.575	56.901 s
B	1 September 2023-05:06:21.322	1 September 2023-05:07:14.136	52.814 s

According to Figure 8 and Table 2, the time difference between the ground stations is about 390 s, which approximates the 400 s duration in Section 4.1. Additionally, the time windows for establishing links with ground stations A and B are about 56.9 s and 52.8 s, respectively. The time durations are enough for the ground receivers to lock and decode the signal. Therefore, the transmission performance of the inter-satellite link of the local satellite is available.

The evolutions of the off-axis angle and rotation angle of the local satellite’s beam pointing are shown in Figure 9. It can be seen from Figure 9 that the evolutions in the beam pointing angles follow the relative motion of the virtual target satellite with respect to the local satellite. The off-axis angle and rotation angle are about 6.6° and 5.2° when the local satellite links to ground station A, respectively, while for ground station B, the off-axis

angle and rotation angle are about 5.2° and 5.0° , respectively. The rates of change in these angles are acceptable in practical missions.

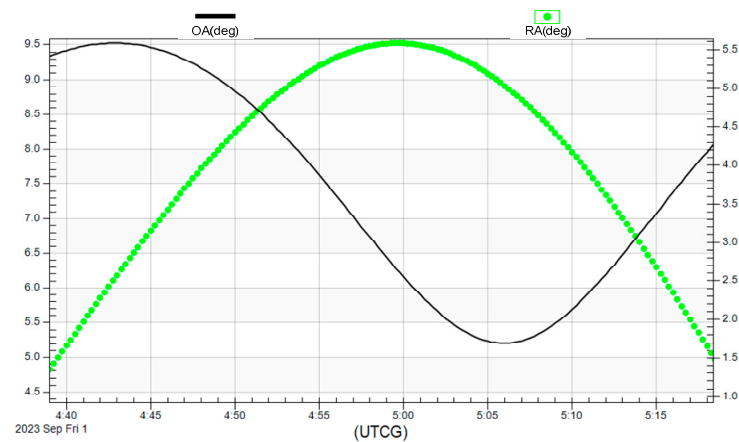


Figure 9. Inter-satellite link pointing to the off-axis angle (OA) and rotation angle (RA) curves.

5. Conclusions

The test method for a single satellite's pointing and tracking abilities with respect to the inter-satellite link is studied. The proposed method is available for multiple types of transmission equipment, such as microwaves and lasers. The rotation angle and off-axis angle for the inter-satellite link pointing and tracking of local and target satellites are derived. The virtual target satellite is simulated by two ground stations. The orbit of the virtual satellite is obtained according to the desired orbital altitude. The time difference between the two ground stations' pointings is solved through several iterations. The pointing and tracking abilities of the local satellite are evaluated by comparing the actual time differences between the ground stations receiving the signals to the theoretical time difference, which achieves an independently in-orbit test of inter-satellite performance.

According to the simulation results, the final error in the time difference in the virtual target satellite is 5 ms, which suggests that two ground stations can simulate the motion of a virtual target satellite. The time windows for establishing links with ground stations A and B are about 56.9 s and 52.8 s, respectively. The off-axis angle and rotation angle for pointing to station A are about 6.6° and 5.2° , while those for pointing to station B are about 5.2° and 5.0° , respectively. Considering a 0.3° half-beam angle, the time difference is about 390 s, which approximates the theoretical value of 400 s. These results demonstrate that the pointing and tracking abilities of the satellite satisfy the demands for establishing an inter-satellite link.

Author Contributions: Methodology, Z.H., L.Y. and S.L.; Software, Z.H., Z.B. and Y.Y.; Validation, Z.B.; Investigation, Z.H., X.H., L.Y. and Y.Y.; Writing—original draft, X.H.; Supervision, S.L. All authors have read and agreed to the published version of the manuscript.

Funding: This work was funded by Science and Technology on Space Intelligent Control Laboratory (Grant Nos. HTKJ2024KL502001 and HTKJ2024KL502006).

Data Availability Statement: Data is contained within the article.

Conflicts of Interest: The authors declare no conflict of interest.

References

- Buzzi, P.G.; Selva, D. Evolutionary formulations for design of heterogeneous earth observing constellations. In Proceedings of the 2020 IEEE Aerospace Conference, Big Sky, MT, USA, 7–14 March 2020; IEEE: New York, NY, USA, 2020; pp. 1–10.
- Gu, X.; Bai, J.; Zhang, C.; Gao, H. Study on TT&C resources scheduling technique based on inter-satellite link. *Acta Astronaut.* **2014**, *104*, 26–32.
- Liu, X.; Zhao, Z.; Li, X.; Leng, T.; Chen, M. Research status and key technologies analysis of inter-satellite link. *J. Telem. Track. Command.* **2019**, *40*, 1–9.

4. Chen, Q.; Giambene, G.G.; Yang, L.; Fan, C.; Chen, X. Analysis of inter-satellite link paths for LEO mega-constellation networks. *IEEE Trans. Veh. Technol.* **2021**, *70*, 2743–2755. [[CrossRef](#)]
5. Li, H.; Gu, X. Design of multilayered satellite communication networks and geometrical analysis of ISLs. *J. Astronaut.* **2005**, *26*, 59–64, 69.
6. Lin, Y.; Qin, Z.; Chu, H.; Wang, H. A satellite cross link-based GNSS distributed autonomous orbit determination algorithm. *J. Astronaut.* **2010**, *31*, 2088–2094.
7. Lin, Y.; He, S.; Zheng, J.; Chu, H. Development recommendation of inter-satellites links in GNSS. *Spacecr. Eng.* **2010**, *19*, 1–7.
8. Fernandez, F.A. Inter-satellite ranging and inter-satellite communication links for enhancing GNSS satellite broadcast navigation data. *Adv. Space Res.* **2011**, *47*, 786–801. [[CrossRef](#)]
9. Zhang, R.; Tu, R.; Fan, L.; Zhang, P.; Liu, J.; Han, J.; Lu, X. Contribution analysis of inter-satellite ranging observation to BDS-2 satellite orbit determination based on regional tracking stations. *Acta Astronaut.* **2019**, *164*, 297–310. [[CrossRef](#)]
10. Xie, X.; Geng, T.; Ma, Z.; Chen, L.; Liu, J. Estimation and analysis of BDS-3 satellite yaw attitude using inter-satellite link observations. *GPS Solut.* **2022**, *26*, 106. [[CrossRef](#)]
11. Zhang, R.; Tu, R.; Zhang, P.; Fan, L.; Han, J.; Lu, X. Orbit determination of BDS-3 satellite based on regional ground tracking station and inter-satellite link observations. *Adv. Space Res.* **2021**, *67*, 4011–4024. [[CrossRef](#)]
12. Kur, T.; Liwosz, T.; Kalarus, M. The application of inter-satellite links connectivity schemes in various satellite navigation systems for orbit and clock corrections determination: Simulation study. *Acta Geod. Geophys.* **2021**, *56*, 1–28. [[CrossRef](#)]
13. Michalak, G.; Glaser, S.; Neumayer, K.H.; König, R. Precise orbit and Earth parameter determination supported by LEO satellites, inter-satellite links and synchronized clocks of a future GNSS. *Adv. Space Res.* **2021**, *68*, 4753–4782. [[CrossRef](#)]
14. Sajjad, N.; Mirshams, M.; Hein, A.M. Spaceborne and ground-based sensor collaboration: Advancing resident space objects' orbit determination for space sustainability. *Astrodynamics* **2024**, *8*, 325–347. [[CrossRef](#)]
15. Zhang, C.; Chen, Q.; Tang, Z.; Wei, J.; Liu, G. Pre-coded inter-satellite routing algorithm with load balancing for mega-constellation networks. *Space Sci. Technol.* **2024**, *4*, 0103. [[CrossRef](#)]
16. Heine, F.; Kämpfner, H.; Czichy, R.; Meyer, R.; Lutzer, M. Optical inter-satellite communication operational. In Proceedings of the 2010 IEEE Military Communications Conference, San Jose, CA, USA, 31 October–3 November 2010; pp. 1583–1587.
17. Gregory, M.; Heine, F.; Kämpfner, H.; Lange, R.; Lutzer, M.; Meyer, R. Commercial optical inter-satellite communication at high data rates. *Opt. Eng.* **2012**, *51*, 1202–1209. [[CrossRef](#)]
18. Zhao, J.; Zhao, S.; Li, Y.; Zhao, W.; Han, L.; Li, X. Advance on data relay technology for inter-satellite laser links. *Infrared Laser Eng.* **2013**, *42*, 3103–3110.
19. Schlicht, A.; Marz, S.; Stetter, M.; Hugentobler, U.; Schäfer, W. Galileo POD using optical inter-satellite links: A simulation study. *Adv. Space Res.* **2020**, *66*, 1558–1570. [[CrossRef](#)]
20. Jia, H.; Bao, W.; Rong, W.; Yu, L.; Xue, X.; Fan, J. Numerical Study on Aerodynamic Characteristics of Parachute Models for Future Jupiter Exploration. *Space Sci. Technol.* **2024**, *4*, 0116. [[CrossRef](#)]
21. Scheinfeild, M.; Kopeika, N.S.; Melamed, R. Acquisition system for microsattellites laser communication in space. *Proc. Spie Int. Soc. Opt. Eng.* **2000**, *3932*, 166–175.
22. Teng, Y.; Wang, Y.; Chen, J.; Feng, X.; Li, X. Inter-satellite link directivity algorithm research and performance validation. *Chin. J. Sci. Instrum.* **2014**, *35*, 96–100.
23. Nielsen, T.T. In orbit test result of an operational intersatellite link between ARTEMIS and SPOT4. In *Free-Space Laser Communication Technologies XIV*; SPIE: San Francisco, CA, USA, 2002; Volume 4635, pp. 1–15.
24. Lin, Y.; Cheng, J.; He, S.; Wang, H. Review on fast acquisition techniques of laser inter-satellite links. *Spacecr. Eng.* **2018**, *27*, 102–109.
25. Guo, S.; Zhou, W.; Zhang, J.; Sun, F.; Yu, D. Integrated constellation design and deployment method for a regional augmented navigation satellite system using piggyback launches. *Astrodynamics* **2021**, *5*, 49–60. [[CrossRef](#)]
26. Li, Z.; Long, T.; Zhao, B.; Qiu, W. The Node Security Access Authentication Method for Mega-Constellation based on Sharding Blockchain. *Space Sci. Technol.* **2024**, *4*, 0143. [[CrossRef](#)]
27. Hui, T.; Zhai, S.; Zhang, Z.; Liu, C.; Gong, X.; Ni, Z.; Yang, K. A High-Precision Satellite Ground Synchronization Technology in Satellite Beam Hopping Communication. *Space Sci. Technol.* **2024**, *4*, 47. [[CrossRef](#)]

Disclaimer/Publisher's Note: The statements, opinions and data contained in all publications are solely those of the individual author(s) and contributor(s) and not of MDPI and/or the editor(s). MDPI and/or the editor(s) disclaim responsibility for any injury to people or property resulting from any ideas, methods, instructions or products referred to in the content.